



Friction and Work Function Oscillatory Behavior for Even and Odd Number of Layers in Polycrystalline MoS₂

Journal:	<i>Nanoscale</i>
Manuscript ID	NR-ART-01-2018-000238.R1
Article Type:	Paper
Date Submitted by the Author:	20-Mar-2018
Complete List of Authors:	Lavini, Francesco ; CUNY Advanced Science Research Center Calo, Annalisa; CUNY Advanced Science Research Center, Gao, Yang; CUNY Advanced Science Research Center Albisetti, Edoardo; CUNY Advanced Science Research Center Li, Tai-De; CUNY Advanced Science Research Center Cao, Tengfei; City University of New York Graduate School and University Center Li, Guoqing; North Carolina State University College of Engineering Cao, Linyou; North Carolina State University College of Engineering Aruta, Carmela; CNR-SPIN, Area della Ricerca di Roma 2 - "Tor Vergata" Riedo, Elisa; CUNY Advanced Science Research Center

Friction and Work Function Oscillatory Behavior for Even and Odd Number of Layers in Polycrystalline MoS₂

Francesco Lavini^{1,2,3†}, Annalisa Calò^{1,3†}, Yang Gao¹, Edoardo Albisetti^{1,4}, Tai-De Li¹, Tengfei Cao^{2,5}, Guoqing Li⁶, Linyou Cao^{6,7}, Carmela Aruta^{1,8*}, and Elisa Riedo^{1,2,3,9*}

¹Advanced Science Research Center, City University of New York, 85 St Nicholas Terrace, New York, New York 10031, USA

²CUNY Graduate Center, Ph.D. Program in Physics and Chemistry, New York, NY 10016

³Tandon School of Engineering, NYU, New York, NY

⁴Dipartimento di Fisica, Politecnico di Milano, Via Giuseppe Colombo 81, 20133, Milano, Italy

⁵Department of Chemistry, College of Staten Island, City University of New York, 2800 Victory Boulevard, Staten Island, New York 10314, USA

⁶Department of Materials Science and Engineering, North Carolina State University, Raleigh, NC 27695

⁷Department of Physics, North Carolina State University, Raleigh, NC 27695

⁸National Research Council CNR-SPIN, Viale del Politecnico 1, I-00133, Rome, Italy

⁹Physics Department, City College of New York, City University of New York, Marshak Science Building, 160 Convent Avenue, New York, New York 10031, USA

* Corresponding author: elisa.riedo@nyu.edu, carmela.aruta@spin.cnr.it

† These authors contribute equally to this work.

A large effort is underway to investigate the properties of two-dimensional (2D) materials for their potential to become building blocks in a variety of integrated nanodevices. In particular, the ability to understand the relationship between friction, adhesion, electric charges and defects in 2D materials is of key importance for their assembly and use in nano-electro-mechanical and energy harvesting systems. Here, we report on a new oscillatory behavior of nanoscopic friction in continuous polycrystalline MoS₂ films for odd and even number of atomic layers, where odd layers show higher friction and lower work function. Friction force microscopy combined with Kelvin probe force microscopy and X-ray photoelectron spectroscopy demonstrate that an enhanced adsorption of charges and OH molecules is at the origin of the observed increase in friction for 1 and 3 polycrystalline MoS₂ layers. In polycrystalline films with an odd number of layers, each crystalline nano-grain carries a dipole due to the MoS₂ piezoelectricity, therefore charged molecules adsorb at the grain boundaries all over the surface of the continuous MoS₂ film. Their displacement during the sliding of a nano-size tip gives rise to the observed enhanced dissipation and larger nanoscale friction for odd layer-numbers. Similarly, charged adsorbed molecules are responsible for the work function decrease in odd layer-number.

Introduction

The ability to manipulate, control and investigate with nanoscopic precision atomically thin sheets of a variety of 2D materials(1, 2) from graphene(3, 4) to transition metal dichalcogenides (TMDC) such as MoS₂(5-7), has opened the route for observing and understanding new fascinating physical properties, and for their practical use in several device technologies(8-10). 2D materials also offer the opportunity to shed light into the molecular mechanisms underlying friction(11-18), one of the oldest, complex and still pressing problem in a variety of industrial applications today, from automotive/transportation industry to microelectromechanical systems (MEMS). Beside the fundamental scientific interest, 2D materials and in particular MoS₂ have many potential applications in nanoelectromechanical systems (NEMS)(12, 19, 20), lubrication, energy harvesting(21, 22), and flexible electronics devices(10). For all these applications,

it is very important to comprehend the tribological behavior of MoS₂ when reduced to 2D thin film scale. A characteristic unique frictional behavior has been recently found in 2D exfoliated single crystal flakes of MoS₂, where friction forces decrease when increasing the number of atomic layers, approaching the value of the bulk case(13). This behavior was believed to be universal for 2D materials and was explained as due to a puckering effect, where adhesion to a sliding probe creates out-of-plane deformations of thinner sheets, leading to increased contact area and, hence, friction. Nevertheless, it remains unclear if the same model applies for extended continuous polycrystalline 2D films, grown for example by chemical vapor deposition (CVD), which are very attractive for large scale industrial applications and MEMS fabrication(23).

Here we show a new, very different frictional behavior for atomically thin continuous films of polycrystalline MoS₂ grown by CVD(5), which is not observable in single crystal MoS₂. In particular, for polycrystalline MoS₂ we observe an oscillatory behavior with higher friction for odd number of layers and lower friction for even number of layers. We perform atomic force microscopy (AFM) based friction force microscopy (FFM) measurements at different humidity, combined with Kelvin probe force microscopy (KPFM) and X-Ray photoelectron spectroscopy (XPS) and we demonstrate that an enhanced adsorption of charges and charged molecules all over the surface of polycrystalline MoS₂ films with an odd number of layers is at the origin of the observed increase in friction for 1 and 3 layers (1L, 3L) in ambient conditions. In particular, XPS demonstrates an enhanced adsorption of hydroxyl species at the surface of polycrystalline MoS₂ films containing an odd number of layers, a fact that shifts the Fermi energy towards the conduction band, lowering the work function of the odd layers, as determined by KPFM. It is well known in literature(21, 22) that single crystal MoS₂ flakes with an odd number of layers are piezoelectric with a net in-plane polarization that can be neutralized by free charges or molecules adsorbed at the edges of the flakes. On the other hand, in a polycrystalline film with an odd number of layers, each nano-crystalline grain carries a dipole that attracts charges and charged molecules at the grain boundaries (GB) present all over the surface (see Fig. 1). These charges and charged molecules, present only on the surface of 1L and 3L polycrystalline MoS₂ samples, are displaced during the sliding of the AFM tip on the MoS₂ surface in friction experiments, giving rise to an

enhanced dissipation and larger frictional forces in odd layer-number. Friction at the micro- and nanoscale in a FFM experiment is dominated by short-range interactions between the sliding tip and the surface. Indeed, being an energy-dissipating process, it strongly depends on the potential energy landscape of the tip-surface interactions(24, 25), and literature shows several examples of the key role of charges and electronic dissipation in sliding friction(26, 27). This oscillatory friction behavior is not present in the large micron-size single crystal MoS₂ triangular flakes containing 1 or 3 layers, where charges are present only at the crystal edges, which are several micrometers apart, having a negligible impact on nanoscale friction.

Experimental Section

CVD Polycrystalline and Single Crystal MoS₂ films. Growing uniform and continuous MoS₂ thin films over large areas, additionally controlling the number of layers, is challenging because MoS₂ monolayers coexist with by-products with higher thickness. In this work continuous polycrystalline 1 cm² MoS₂ films are used, which are produced following a recently developed approach(5). Briefly, molybdenum chloride (MoCl₅) powder (99.99%, Sigma-Aldrich) is placed at the center of the furnace and sulfur powder (Sigma-Aldrich) at the upstream entry of the furnace. Receiving substrates (sapphire, Al₂O₃) is placed in the downstream of the tube. Typical growth conditions include a temperature of 850°C, a flow rate of 50 SCCM, and a pressure of about 2 Torr. The thickness of the film can be precisely controlled by changing the amount of MoCl₅. In our study, we analyze four types of polycrystalline MoS₂ films with defined thickness, from 1 to 4 atomic layers. Crystalline quality and thickness are characterized by AFM, STEM and Raman spectroscopy (see Supporting Information, Fig. S1-S3).

For comparison, we also investigate MoS₂ single crystals of ~ 1 μm size, also grown by CVD on sapphire according to a reported procedure(28-30). Using MoO₃ together with S powders as precursors allows the growth of MoS₂ single crystals with characteristic triangular shapes. In particular, the excess of Mo precursor enhances the vertical growth, with thicknesses progressively ranging from one to several atomic layers (10L).

Friction Force Microscopy. Friction Force Microscopy measurements, together with topography imaging, are performed in contact mode with a Bruker Multimode 8 AFM. We use silicon AFM probes (PPP-CONT Nanosensor) with normal spring constant k between 0.2-0.4 N/m, calibrated using the thermal noise method(31). The lateral spring constant is obtained from the normal one using a conventional relationship for a rectangular cantilever(32) (more details are reported in the Supporting Information). We underline that, although the spring constant is carefully calibrated, small changes in the tip size may vary the absolute value of the measured friction forces. For this reason, we follow the procedure of always measuring friction forces from a reference sample before and after each new measurement on MoS₂ films. In particular, freshly cleaved bulk MoS₂ is measured at the beginning and at the end of each set of experiments as a reference for the absolute values of friction, to ensure reliability in the comparison between samples at different number of layers. Our experiments are performed on three batches of polycrystalline MoS₂ films, where each batch includes four films, with atomic thicknesses of 1, 2, 3, and 4 layers, along with several different single crystal MoS₂ structures with the same thicknesses. During each series of friction measurement, we scan each sample over a $1 \times 0.5 \mu\text{m}^2$ area, with a scanning speed of $2 \mu\text{m/s}$ (1 Hz), collecting data at different normal loads, from 3 nN to 18 nN, on multiple positions of each sample. Each reported friction data point per load and per individual sample (i.e. polycrystalline or single crystal, with a given number of layers) therefore represents the average value over 9 different series and forty different measurements. Finally, each complete series of friction experiments, comparing 1L to 4L polycrystalline films and single crystal, as well as bulk MoS₂, in humid and dry conditions is usually performed within the same day to ensure the same conditions for tip and environment. After collecting friction scans in humid environment ($\text{RH} = 45 \pm 5\%$), at 15 nN normal load, we bring the scanning environment to low relative humidity ($\text{RH} \approx 5\%$), and perform an entire set of friction force measurement. This procedure is standardized for all samples. If the friction measurements on the reference MoS₂ bulk sample suggest that the tip has changed properties or has been damaged, the whole set of experiments is discarded. During friction measurements performed in humid conditions, relative humidity (RH) is constantly monitored to be $45 \pm 5\%$. For measurements in dry conditions, RH is kept

around 5% by using an AFM fluid cell and flowing nitrogen gas (N_2) in it for 15 minutes, and let the environment in the cell rest for other 5/10 minutes, to stabilize the measurements system. Before conducting the experiments in dry conditions, we perform some scans in humid conditions for each sample, within the same range of normal loads. In this way, it is possible to observe directly the variation of friction forces with relative humidity.

X-Ray photoelectron spectroscopy (XPS). X-ray photoelectron spectroscopy (XPS) measurements are used to analyze the chemical configuration of the samples, including their valence states. Measurements are performed with the Physical Electronics VersaProbe II using Al $K\alpha$ radiation (1486.6 eV). We collect Mo $3d$, S $2p$, and O $1s$ core level spectra for all polycrystalline samples, from 1L to 4L, to study the influence of thickness on the binding energies and composition. We also measure the valence band spectra by finely scanning close to the Fermi edge, where binding energy is zero. More details about the measurements and the fitting procedure are provided in the Supporting Information (Fig. S4-S6). As mentioned above, the characteristic dimension of the MoS_2 single crystals used in our study is about $1\mu m$, and the distribution and density of the crystals on the surface is such that crystals of different, random thickness can be found within the same micrometer-size area (see Figs. S2c-e of the Supporting Information). Since the lateral spatial resolution used during the XPS experiments is about $200\mu m$, it is impossible to isolate crystals with only one population of thickness. Mo $3d$ and S $2p$ core level spectra, resulting from the contributions of single crystals with different thicknesses are reported in the SI in Fig. S4.

Kelvin Probe Force Microscopy (KPFM). Frequency-modulated Kelvin Probe Force Microscopy (FM-KPFM) experiments are performed with the same Bruker Multimode 8 AFM used for friction measurements and using Pt/Ir coated cantilevers with resonance frequency $f \sim 75$ kHz and spring constant 0.5-10 N/m (PPP-EFM Nanosensors). Polycrystalline and single crystal CVD MoS_2 samples (size = 0.5×0.5 cm²) are glued on metallic sample holder disks with conductive tape and then additionally connected to the sample holders with silver paste. Topography and KPFM images ($2 \times 2\mu m^2$, 512×512

pixels) are collected at a scan rate of 0.2 Hz for polycrystalline MoS₂ samples, while 256 x 256 pixels images are collected at a scan rate of 1 Hz for single crystal MoS₂ samples. The amplitude of the AC voltage used for FM-KPFM measurements is set at 4 V in order to ensure low-noise FM-KPFM images while avoiding artifacts in the AFM topography. The work function (W_F) of MoS₂ samples is obtained from contact potential difference (CPD) images according to the following equation: $W_F^{\text{MoS}_2} = W_F^{\text{tip}} + e \cdot \text{CPD}$, where e is the electronic charge and W_F^{tip} is extracted from the CPD images of a gold calibration sample, assuming $W_F^{\text{gold}} = 5.1$ V(33, 34) (see Fig. S9 of the Supporting Information). For the polycrystalline samples, $W_F^{\text{MoS}_2}$ (average value and standard deviation) is obtained from a Gaussian fit of the normalized distribution histogram from the KPFM images shown in Fig. 4d and S7 of the Supporting Information. Each histogram shows the number density of pixels at each W_F vs. the corresponding W_F . For single crystal samples, $W_F^{\text{MoS}_2}$ (average value and standard deviation) is obtained from the average and RMS values of CPD taken on rectangular areas inside each crystal of a certain thickness, from 1L to 10L (KPFM images are shown in Fig. S8b and d of the Supporting Information).

Results and discussion

In the present study, we use atomic force microscopy (AFM) to explore the friction behavior of continuous polycrystalline films of MoS₂ (Fig. 1a), which are grown by CVD on sapphire(5) (see also the Experimental Section and the Supporting Information SI). MoCl₅ and sulfur powder are used as precursors to obtain a self-limiting deposition with a superficial, rather than vertical growth, leading to large area (1x1 cm²), atomically thin polycrystalline samples of uniform thickness. These MoS₂ films contain crystalline grains varying from tens to hundreds of nanometers, which are observable in AFM and in transmission electron microscopy (TEM) images (Fig. 1a and 1d). In our study, we analyze polycrystalline MoS₂ samples with four different thicknesses, namely 1, 2, 3, and 4 atomic layers. Vertical alignment of the layers is explored via scanning transmission electron microscopy (STEM). High-angle annular dark field (HAADF) images of MoS₂ mono- and bilayer films (Fig. 1e and 1f, respectively) show a substantial difference in their lattice orientation, indicating an AB stacking sequence in the bilayer, where Mo

atoms of the top layer overlap with the sites of S atoms in the underlying layer. Because of its crystal structure, a single layer of MoS₂ shows a broken inversion symmetry associated with a net in-plane permanent polarization (see Fig. 1b)(21); while no net in-plane permanent polarization is present in the symmetric even layers, e.g. 2, 4 layers (Fig. 1c). Therefore the layers alignment inside each grain very likely gives rise to a net in-plane dipole in each grain in odd-numbered layers, and its disappearance for even-numbered layers. Samples are characterized by AFM topography, Raman spectroscopy and electron microscopy, as reported in the Supporting Information (Fig. S1-S3).

For comparison, we also investigate MoS₂ single crystals with characteristic triangular shapes of micrometer size, also grown by CVD on sapphire(28-30). In particular, the excess of Mo precursor in this method enhances the vertical growth of each single crystal, with thicknesses progressively ranging from one to several atomic layers (10L). Thus, these MoS₂ structures also exhibit 1L, 2L, 3L, and 4L crystals of few micrometer size that can be easily distinguished in AFM images and serve as a comparison with polycrystalline samples. An AFM image of a 1L MoS₂ single crystal is shown in the inset of Fig. 2b.

Figures 2a and 2b show the average friction force as a function of the number of atomic layers, obtained from FFM experiments performed in humid environment (relative humidity RH = 45%) on polycrystalline MoS₂ films and on MoS₂ single crystals respectively. The friction values are extracted from 1 x 0.5 μm² area friction images and averaged over more than 40 measurements for each load and sample, see experimental section for more details. Graphs are obtained normalizing friction values of the different samples with the ones obtained for freshly cleaved bulk MoS₂. Figures 2a and 2b clearly show a different behavior between MoS₂ polycrystalline films and single crystals, as friction forces in ambient conditions are significantly larger for the former compared to the latter. Furthermore, very interestingly, while friction on single crystal MoS₂ monotonically decreases as a function of thickness, as previously observed in literature for single crystal MoS₂ flakes(13), on polycrystalline films we observe an oscillatory behavior with higher friction forces for 1L and 3L (odd-numbered layers) and smaller friction forces for 2L and 4L (even-numbered layers). This oscillation is superimposed to a monotonic downward trend towards the bulk value.

We remark that in Figure 2a we show the average friction force values obtained from 9 different series of experiments on polycrystalline MoS₂ films with four different thicknesses, for a total of 36 series, and each of these 9 series includes friction experiments for films with 1, 2, 3, 4 layers, where these four films for each series are previously grown in the same 24-48 hours' time-window. Specifically, three different "batches" of samples have been investigated, such that we performed 4 series of experiments on batch #1 (1, 2, 3, 4 L), 3 series on batch #2 (1, 2, 3, 4 L) and 2 series on batch #3 (1, 2, 3, 4 L). Furthermore, each series of friction experiments includes several measurements in different regions of the surface for each number of layers and each series follows a given random sequence in terms of the order in which the samples are measured. Because we measure three different batches of samples, and 9 different series over a period of one year, the friction standard deviation for each thickness displayed in Fig. 2a and calculated over all the measurements (~40 for each thickness) is quite large; however it is important to underline that the oscillatory friction behavior is present for each of the three batches of samples, and more generally for each of the 9 series. For example, we show in Fig. 2c the normalized friction force values from 3 different series, each corresponding to one of the 3-different batches of samples, showing a clear oscillatory friction behavior with the number of layers. The relative error bar shown in this figure corresponds to the deviation of friction values within different regions of the same sample. It is thus clear how the oscillatory behavior is a property of polycrystalline MoS₂ and does not depend on the conditions of the single experiment or on the batch of samples used. For comparison, we also show three different series of measurements on single crystal MoS₂ samples in Fig. 2d.

The observed variation of the friction force with number of layers in polycrystalline MoS₂ films can have different explanations. The friction force (F_F) at the nanoscale is related to the friction coefficient (μ), the adhesion force (F_{adh}) and the normal forces (F_N). In first approximation and in the range of loads we are considering, F_F is given by the following Equation(18, 35) :

$$F_F = \mu (F_N + F_{adh}) \quad (1)$$

To understand the origin of the observed friction oscillations in polycrystalline MoS₂ films, we measure the friction forces as a function of the normal applied load for each

sample at the same RH = 45%. Results are shown in Fig. 2e. For comparison, the same measurements are also performed on single crystal MoS₂ triangular structures, under the same conditions (see Fig. 2f). The friction data for each type of sample are fitted with a linear fit, according to Equation 1. Extracted μ and F_{adh} are reported in Table 1 and in the Table S3 of the Supporting Information, respectively. The fitting procedure shows that for MoS₂ single crystals the friction coefficient monotonically decrease when increasing the thickness, approaching the low values of the bulk MoS₂ for $L > 4$. This decrease is in agreement with previous results on MoS₂ single crystal flakes(13). It was also previously shown that for exfoliated single crystal MoS₂ the adhesion force does not critically change with atomic thickness(13), and this result is in agreement with our findings for single crystal MoS₂ (see Table S3 of the SI, right column). On the other hand, for the polycrystalline films, friction coefficients are higher for 1L and 3L compared to 2L and 4L (see Table 1), showing that superimposed to the previously observed monotonic downward trend towards the bulk value, we observe an oscillatory behavior between odd and even number of layers. Regarding the adhesion forces, we did not observe any clear dependence of the measured F_{adh} on the number of layers for polycrystalline MoS₂ samples. Thus, adhesion seems to be unrelated to the observed oscillatory trend of F_F in polycrystalline MoS₂. For polycrystalline samples (Table S3 of SI, left column), we notice that the 1L sample displays a significantly lower value of adhesion force compared to the thicker samples. It may be possible that in this case high density of negative charged particles concentrated on the film surface (see further in the text) change the contact between tip and surface through the effect of electrostatic forces. Indeed, it has been observed that adhesion force decreases with increasing concentration of OH⁻ on the surface of metals and semiconductors, generating a repulsive component that directly affects the tip contact(36). We also fit the friction data accordingly with the single-asperity 2/3 power law equation(37) (see Table S2 of the SI), obtaining the same conclusions.

To further explore the origin of the frictional behavior of polycrystalline MoS₂, we perform FFM friction experiments in dry conditions (RH \approx 5%) (see Fig. 3). In dry conditions, the oscillatory friction behavior disappears and polycrystalline MoS₂ behaves

as the single crystal sample, showing a monotonic decaying trend of F_F vs. number of layers, as it can be seen comparing Fig. 3a and 3b. We conclude that the humid environment is crucial in sustaining the new and very interesting oscillatory behavior observed in polycrystalline MoS_2 for even or odd number of atomic layers.

Here, we propose that the friction oscillatory behavior is related to the odd layer-numbers in-plane piezoelectricity that has been previously demonstrated in MoS_2 single crystal flakes(21, 22). Indeed, because of its crystal structure, MoS_2 shows a broken inversion symmetry when the film presents an odd number of layers, e.g. 1 and 3, with an associated net in-plane permanent polarization (see Fig. 1b)(21); while no piezoelectricity is measured for the symmetric even layers, here 2 and 4 layers (Fig. 1c). For single crystal MoS_2 , the in-plane net permanent polarization produces uncompensated electric fields and local charges only at the flakes edges, and not all over the flake's surface, therefore these charges do not impact the friction interactions between the tip and the surface. However, in the case of a polycrystalline film, each odd layer-number nanocrystalline grain (~ 100 nm in size) of the continuous film displays an in-plane dipole, having a random direction, giving rise to uncompensated electric fields at the grain boundaries which attract charges and adsorbed molecules (see the sketch in Fig. 1g). The humid environment is a source of these charges and charged molecules, such as OH^- , while in dry conditions water concentration drops largely, together with that of such particles(38). During a friction experiment, when the AFM tip slides on the surface of a polycrystalline odd layer-numbers MoS_2 film, the displacement of these charged molecules on the surface gives rise to an enhanced dissipation and larger frictional forces in odd layer-number films. Friction at the micro- and nanoscale is dominated by short-range interactions between the sliding tip and the surface. Thus, being an energy-dissipating process, it strongly depends on the potential energy landscape of the tip-surface interactions(24, 25). Several studies show examples of the key role of charges and electronic dissipation in sliding friction(26, 27). Hereof, the observation of larger friction for odd-numbered layers samples, compared to the case of non-polar grains when the number of layers is even and no charged molecules are likely adsorbed on the surface, or at least in less amount.

Finally, the high density of GB in polycrystalline samples(39) (see the AFM images in Fig. 1a, 2a (inset)) compared to the monocrystalline case (Fig. 2c (inset)) may explain the overall higher value of friction forces generally recorded in the case of all polycrystalline samples compared to single crystals. GB are generally a source of defects(40), and thus represent preferential sites for the localization of adsorbates from the environment in all the polycrystalline samples(41), which as previously discussed increase the friction forces. Accordingly, once in dry environment, the normalized friction in polycrystalline samples becomes comparable to that of single crystals, confirming the predominant effect of adsorbed charges/molecules at the grain boundaries on friction dissipation.

Since it is well known that the presence of local charges and adsorbed molecules can dramatically change the work function of thin films and 2D materials(34, 42-45), to corroborate our picture we perform XPS and KPFM measurements and analyze the variations in the valence band maximum (VBM) and in the work function (W_F) with the number of layers, for both single crystal and polycrystalline MoS₂ samples. We recall that the work function is the energy difference between vacuum level and Fermi energy, while the VBM is the energy difference, considered positive, between the Fermi energy and highest energy level of the valence band; therefore, an upward shift in the Fermi energy corresponds to a decrease in the work function and a corresponding increase in VBM. Figure 4a shows the position of the VBM(46), measured with respect to the Fermi energy (E_F), as a function of the number of layers in the polycrystalline MoS₂. VBM are extracted from the Mo 4d₂₂ band spectra in the XPS measurements (see Fig. S4 of the Supporting Information). Previous VBM(40, 41) and KPFM(33, 47, 48) measurements on MoS₂ as a function of the film thickness showed that the work function of MoS₂ increases with increasing film thickness for two possible reasons. One reason is related to a competing effect between the hole-dopants at the substrate interface³² and the hole-doping molecules adsorbed at the surface, which tend to increase with the thickness due to the screening effect. A second effect is related to the presence of negatively charged surface states, which generate an electric field between surface and substrate amplified for thinner films⁴⁰. Consistently, in our experiments we observe an overall increase of the work function with the number of layers for both single crystal and polycrystalline MoS₂

samples (see Fig. 4c and inset), and a complementary decrease of the VBM in polycrystalline MoS₂ (Fig. 4a). Furthermore, as for the case of friction, in polycrystalline MoS₂ samples we observe an oscillatory behavior related to odd/even number of layers superimposed to the monotonic increase of W_F (decrease of VBM). In particular, the W_F as measured by KPFM is lower for 1L and 3L samples and follows the order $W_F^{1L} < W_F^{3L} < W_F^{2L} < W_F^{4L}$. From our experiments, $W_F^{1L} = 5.01$ eV, $W_F^{2L} = 5.16$ eV, $W_F^{3L} = 5.20$ eV, $W_F^{4L} = 5.29$ eV (Fig. 4c). The average value and the standard deviation of the work function are obtained from distribution histograms extracted from KPFM images collected on polycrystalline MoS₂ with different number of layers (see Fig. 4d and Fig. S7 of the SI). Accordingly, an upward shift in VBM of a few tenths of electron volts is in fact observed in odd layers (1L and 3L). From Fig. 4a, we observe that 1L and 3L films show higher VBM values (~ 1.58 eV and ~ 1.5 eV, respectively) compared to 2L and 4L films (~ 1.42 eV and ~ 1.24 eV, respectively). A similar trend is observed also in the Mo 3*d* and S 2*p* core levels spectra (see Fig. S4 of the SI). Both core levels show the same oscillating shifts, with 1L and 3L samples having higher binding energies compared to 2L and 4L. This indicates that the whole XPS spectrum undergoes a rigid shift(41). Since the binding energies of core levels detected in XPS are referred to the Fermi level of the system, the same observed energy shift can be attributed to a shift in the Fermi energy position, in agreement with the results obtained for the VBM and work function. We attribute the high-energy shift in the core levels of polycrystalline MoS₂ for 1L and 3L to an increased amount of negative charges on the surface(41). Negative charges could be present in the form of quasi-free electrons, originating from S vacancies at the surface or adsorbed OH ions(47) localized at the grain boundaries of each piezoelectric grain as illustrated in Fig. 1g. Both S vacancies and OH molecules are known to increase the n-doping (or decrease the p-doping) character of MoS₂(49-52). Elemental analysis obtained from XPS corroborates this hypothesis, showing an increased amount of hydroxyl OH groups in 1L and 3L polycrystalline MoS₂, as shown in Fig. 4b (see also Fig. S5 of the Supporting Information). Furthermore, we find that the S/Mo ratio for all the polycrystalline samples, as determined from Mo 3*d* and S 2*p* core level spectra, is higher than 2 (see Fig. S6d of the Supporting Information), making unlikely the presence of sulfur vacancies in these samples(33, 53). Therefore, our results indicate that OH

adsorption is the main responsible of the lower p-doping (higher n-doping) character and the corresponding lower work function of polycrystalline MoS₂ with odd number of layers.

For single crystal MoS₂, VBM data are not available, due to the large XPS beam size which cannot resolve single crystals with only one population of thicknesses (further explanation is reported in the XPS experimental section and in the Supporting Information). However, nanoscale KPFM experiments show that W_F monotonically increases with the number of layers, from 4.47 eV for 1L MoS₂ to 5.01 eV for a thick 10L crystal (thickness: 6.5 nm), as shown in the inset of Fig. 4c (corresponding AFM images are shown in Fig. S8 of the Supporting Information). These values are consistent with literature data on MoS₂ single crystals of micrometric size grown by CVD on SiO₂(48) (see Fig. S8 of the Supporting Information). As shown in Fig. 4c, polycrystalline samples exhibit a W_F which is 0.3-0.4 V higher than the monocrystalline counterpart, and even higher than bulk MoS₂ (5.2 eV)(54), indicating a more p-doping character. An explanation for the measured higher values of W_F may come from the stoichiometry of the polycrystalline samples, which contain S excess or Mo vacancies in higher amount compared to the single crystals (see Fig. S4d of the Supporting Information), which are both source of p-doping. Accordingly, XPS Mo 3*d* and S 2*p* core level spectra resulting from the contributions of single crystals with different thicknesses show an overall blue shift (shift towards higher energies) of the binding energies when compared to the polycrystalline MoS₂ films having thicknesses between 1 and 4 L, see Fig. S4 in the SI.

Overall, KPFM and XPS results indicate that the nano-grain-associated dipoles emerging in the odd-numbered layers samples attract negatively charged or electron donor molecules at the grain boundaries, in particular OH⁻, giving rise to the observed larger dissipation in 1L and 3L during the frictional measurements and to a lower W_F and larger VBM for 1 and 3L. Here, the different dipole orientation in the grains affects the charge distribution(55) and reflects into the width of the W_F histograms from KPFM, which is higher for 1L and 3L as compared to 2L and 4L samples (see Fig. 4d).

Conclusions

In conclusion, our study shows a surprising behavior in polycrystalline continuous films of MoS₂, where friction and work function follow an oscillatory variation for odd (high friction, low work function) and even (low friction, high work function) number of layers. These phenomena find explanation in the crystalline structure of MoS₂. For polycrystalline MoS₂ films with odd number of layers, the broken inversion symmetry gives rise to a permanent dipole in each crystalline nano-grain. KPFM and XPS results indicate that the nano-grain-associated dipoles emerging in the odd layers samples attract polar and charged molecules at the grain boundaries. These surface charges change the potential and the sliding energy landscape during tip scanning, giving rise to a larger dissipation in 1L and 3L during the frictional measurements in humid conditions. The same effect is negligible in single crystal MoS₂ structures, where charges are present only at the edges of the large micron-size crystals. Furthermore, being related to the presence of grains in the polycrystalline films structure, we can confidently claim that our observations represent an intrinsic property of polycrystalline MoS₂ 2D layers, rather than being limited to the samples analyzed in this study. Understanding the relationship between friction, charges, and atomic structure may help implementing MEMS devices based on MoS₂, whose use in FETs has already been demonstrated. For example, our study suggests that to reduce adhesion in MoS₂ films it would be appropriate to either use an even number of layers or to treat polycrystalline samples with poling, in order to align electric dipoles. Furthermore, this work indicates how local permanent dipoles may affect the work function of 2D materials, which is one of the key properties for the design of electronic devices based on these materials. Finally, it would be possible to extend these findings to other 2D polycrystalline materials which show similar non center-symmetric structure, like WSe₂.

Associated content

Supporting Information

Supporting Information available. Experimental details on the preparation and growth of polycrystalline MoS₂ samples. Raman, contact-mode AFM and STEM characterization of

polycrystalline MoS₂. Experimental details on FFM measurements. Adhesion forces from linear and power law fitting. Experimental details on XPS measurements and core levels spectra. Tapping-mode and KPFM images of polycrystalline and single crystal MoS₂. Tip calibration for W_F extraction.

Author Information

Corresponding Author

*E-mail: elisa.riedo@nyu.edu, carmela.aruta@spin.cnr.it

Acknowledgments

We acknowledge the support from the Office of Basic Energy Sciences of the US Department of Energy (grant no. DE-SC0016204). We thank Hui-Chun Fu and J. H. He of the King Abdullah University for Science & Technology (KAUST) for providing single crystal CVD samples.

	Polycrystalline	Single Crystal
	μ	μ
1L	0.65 ± 0.03	0.29 ± 0.05
2L	0.20 ± 0.02	0.19 ± 0.06
3L	0.25 ± 0.01	0.10 ± 0.03
4L	0.18 ± 0.02	0.07 ± 0.02
Bulk	0.04 ± 0.01	0.04 ± 0.01

Table 1 | Friction coefficient μ , and corresponding standard deviation as a function of the number of layers, for polycrystalline and single crystal MoS₂ samples.

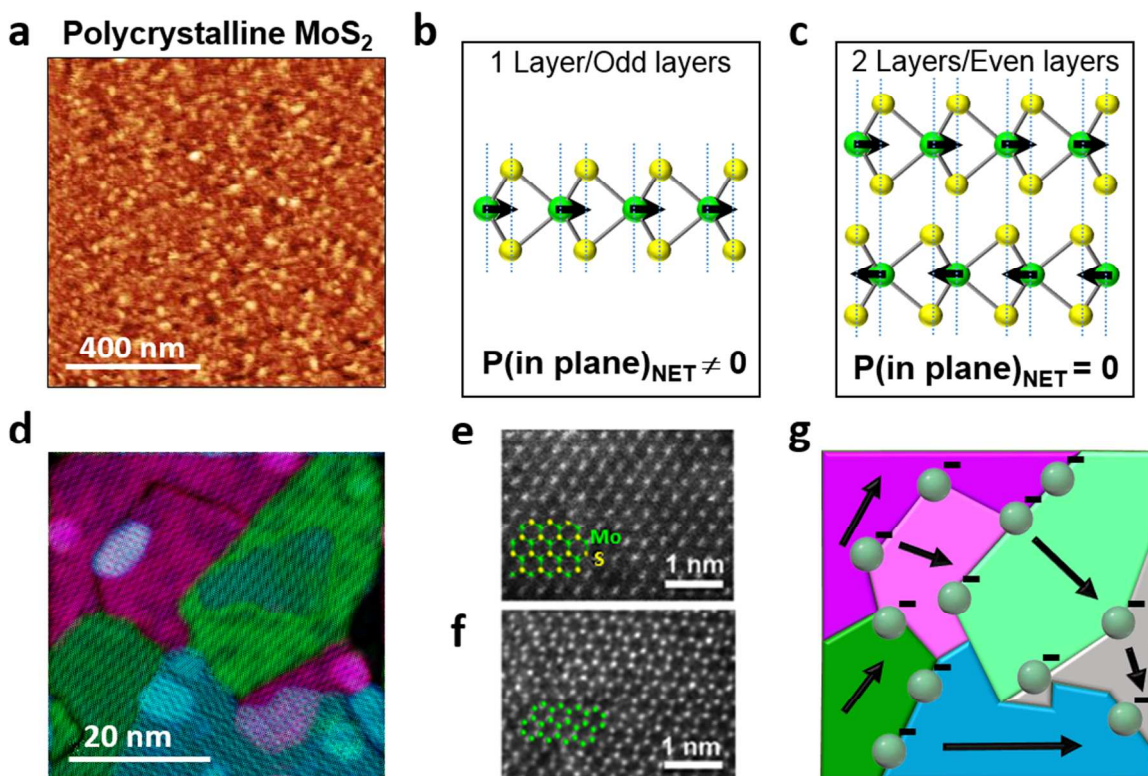


Fig. 1. Schematic representation, TEM, STEM and AFM topography of CVD polycrystalline MoS₂. (a) Contact-mode AFM topography image of polycrystalline MoS₂ single layer film. Grains characteristic dimension varies from tens to hundreds of nanometers. Vertical range scale is between 0 nm and 1.8 nm, and the scan area is 1 μm x 1 μm. (b, c) Schematic representation of one and two molecular layers of MoS₂, respectively, where in-plane dipoles compensate when the number of layers is even. (d) TEM false color image of polycrystalline MoS₂ sample, showing grains of tens of nanometers, with tilt grain boundaries and overlapping grains. (e, f) High-angle annular dark field (HAADF) STEM images of MoS₂ mono- and bilayer films, respectively. Crystal structures are overlapped, with green and yellow dots corresponding to Mo and S atoms, respectively. Fig. 1f is filtered for visual convenience. (g) Schematic representation of the influence of in-plane dipole and grain boundaries on the attraction of charged and polarized particles.

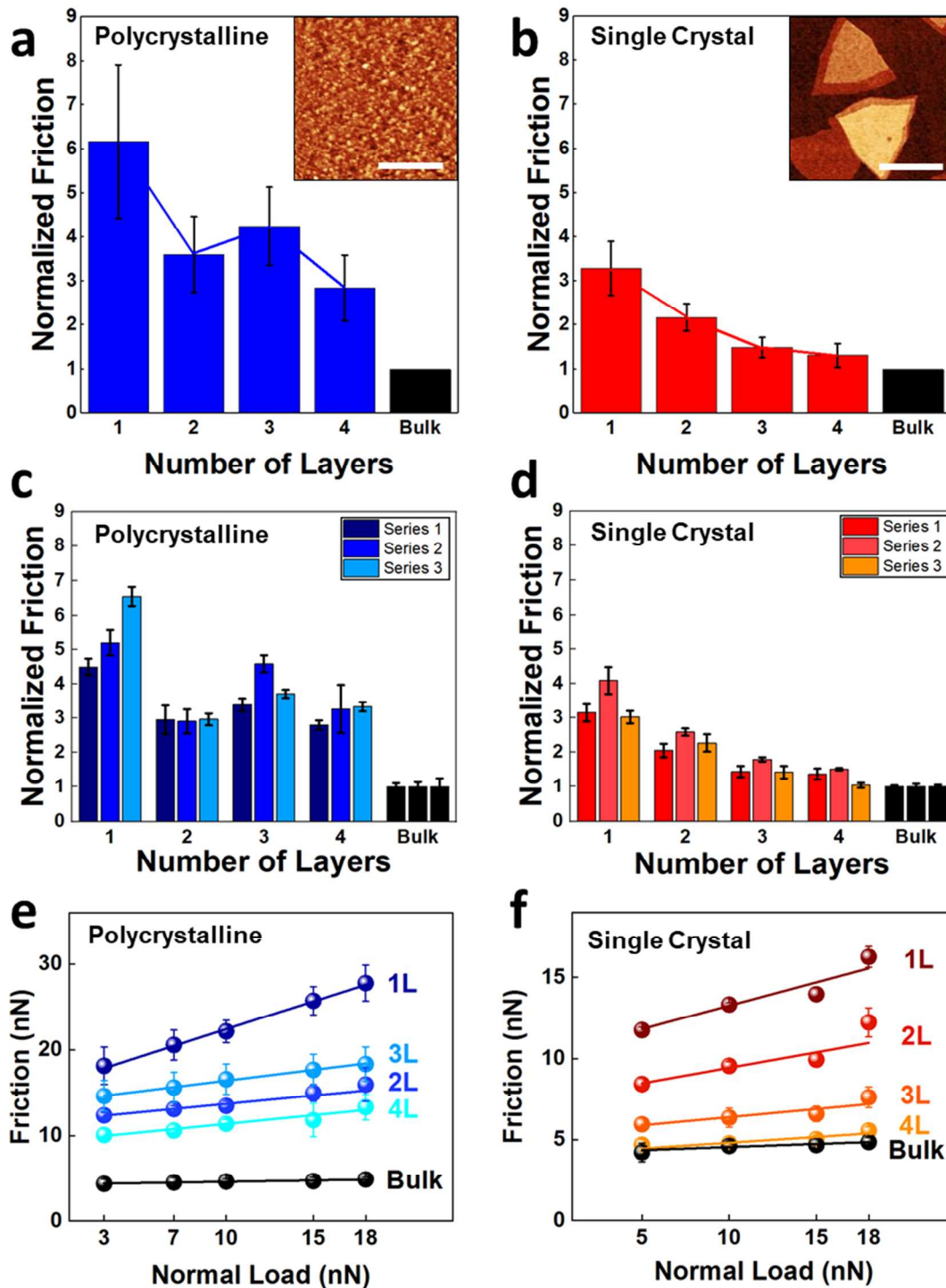


Fig. 2. Friction of single crystal and polycrystalline CVD MoS₂ in humid conditions. (a, b) Evolution of the friction force (normal load 15 nN) with increasing number of atomic layers. For both polycrystalline (a) and single crystal (b) samples, the friction forces are normalized to the value obtained from a MoS₂ bulk reference sample. Insets display corresponding contact-mode

AFM topography images; scale bar is 500nm for both insets. For the case of single crystal MoS₂, the characteristic overlapping of triangular structures can be observed. Vertical scale range is (z scale = 1.8 nm) for inset (a) and (z scale = 3 nm) for inset (b). (c, d) Normalized friction force values (normal load 15 nN) as a function of the number of layers, obtained from 3 different series of experiments, each series obtained from a different batch of samples. (e, f) Friction forces vs. normal load recorded during friction experiments. Each data point and corresponding error bar represents respectively, the average and the standard deviation of the friction values measured on 40 different experiments for each normal load, including different regions per samples, for each number of layers in both single and polycrystalline MoS₂, over three separate batches of samples. For visual accessibility, (e) and (f) have a different ordinate scale.

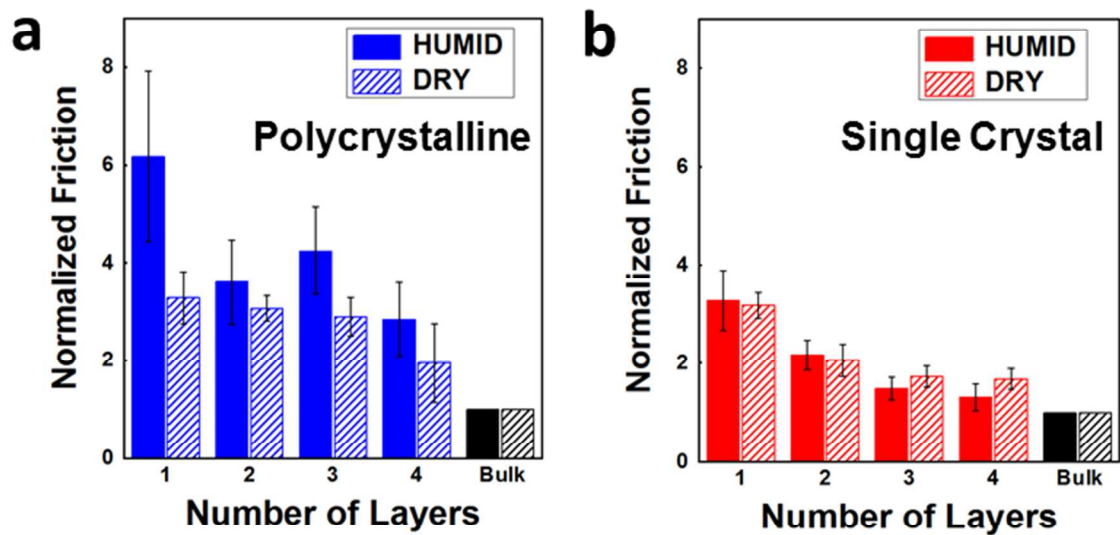


Fig. 3. Comparison of friction forces in humid and in dry conditions. (a, b) Friction force vs. layer thickness in humid ($RH = 45 \pm 5\%$) and in dry environment ($RH \approx 5\%$), at 15 nN normal load, for polycrystalline (a) and single crystal (b) MoS₂. Values are normalized to those obtained for the MoS₂ bulk reference sample, in the same humidity conditions.

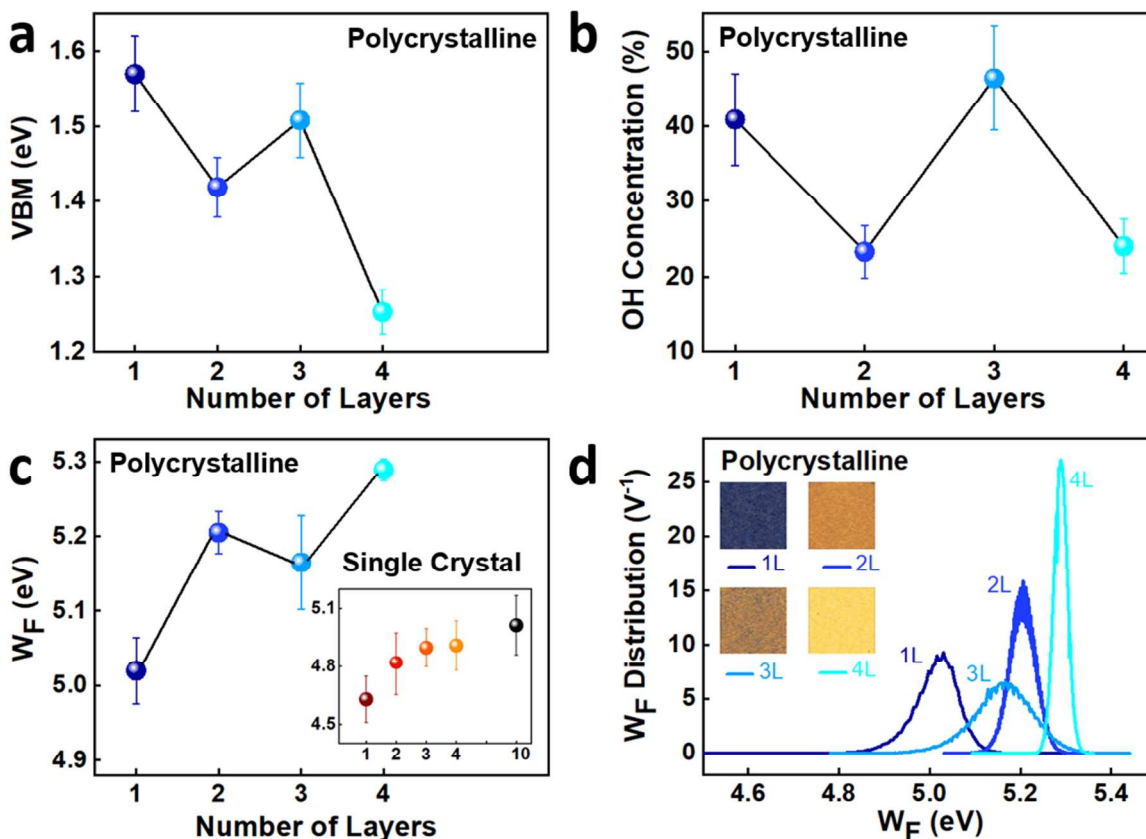


Fig. 4. XPS and Kelvin Probe Force Microscopy of polycrystalline MoS₂. (a) Valence band maximum (VBM) vs. number of atomic layers in polycrystalline MoS₂. (b) Hydroxyl OH concentration, calculated as percent of the whole O 1s spectra (see Supporting Information), vs. number of atomic layers. (c) Work function vs. number of layers for polycrystalline MoS₂ and for single crystal MoS₂ (c, inset). (d) Normalized distribution histograms of the work function values, as extracted from the KPFM images of each polycrystalline MoS₂ sample shown in the same figure. FM-KPFM images show alternating contrast, i.e. higher contact potential difference (CPD) for even layers and lower CPD for odd layers, resulting in brighter and darker images respectively. Images size is 2 x 2 μm² and the vertical scale, identical for all the images, is between -0.25 V and 0.25 V.

References

1. Ramakrishna Matte HSS, Gomathi A, Manna A, K., Late DJ, Datta R, Pati SK, et al. MoS₂ and WS₂ Analogues of Graphene. *Angew Chem Int Ed* 2010;49:4059-62.
2. Park JY, Kwon S, Kim JH. Nanomechanical and Charge Transport Properties of Two - Dimensional Atomic Sheets. *Adv Mater Interfaces*. 2014;1:1300089.
3. Berger C, Song Z, Li X, Wu X, Brown N, Naud C, et al. Electronic Confinement and Coherence in Patterned Epitaxial Graphene. *Science*. 2006;312:1191-6.
4. Kim S, Zhou S, Hu Y, Acik M, Chabal YJ, Berger C, et al. Room-Temperature Metastability of Multilayer Graphene Oxide Films. *Nat Mater*. 2012;11:544-9.
5. Yue Q, Shao ZZ, Chang SL, Li JB. Adsorption of gas molecules on monolayer MoS₂ and effect of applied electric field. *Nanoscale Research Letters*. 2013;8:425.
6. Castellanos-Gomez A, Poot M, Steele GA, van der Zant HSJ, Agraït N, Rubio-Bollinger G. Mechanical Properties of Freely Suspended Semiconducting Graphene-like Layers based on MoS₂. *Nanoscale Res Lett*. 2012;7:233.
7. Jin H-J, Yoon WY, Jo W. Virtual out-of-plane piezoelectric response in MoS₂ layers controlled by ferroelectric polarization. *ACS applied materials & interfaces*. 2017;10(10):1334-9.
8. Zhu Y, Murali S, Stoller MD, Velamakanni A, Piner RD, Ruoff RS. Microwave Assisted Exfoliation and Reduction of Graphite Oxide for Ultracapacitors. *Carbon*. 2010;48:2106-22.
9. Wang X, Zhi L, Müllen K. Transparent, conductive graphene electrodes for dye-sensitized solar cells. *Nano letters*. 2008;8(1):323-7.
10. Lee GH, Yu YJ, Cui X, Petrone N, Lee CH, Choi MS, et al. Flexible and Transparent MoS₂ Field-Effect Transistors on Hexagonal Boron Nitride-Graphene Heterostructures. *ACS nano*. 2013;7:7931-6.
11. Niguès A, Siria A, Vincent P, Poncharal P, Bocquet L. Ultrahigh Interlayer Friction in Multiwalled Boron Nitride Nanotubes. *Nat Mater*. 2014;13:688-93.
12. Kawai S, Benassi A, Gnecco E, Söde H, Pawlak R, Feng X, et al. Superlubricity of Graphene Nanoribbons on Gold Surfaces. *Science*. 2016;351:957-61.
13. Lee C, Li Q, Kalb W, Liu X-Z, Berger H, Carpick RW, et al. Frictional characteristics of atomically thin sheets. *Science*. 2010;328(5974):76-80.
14. Choi JS, Kim J-S, Byun I-S, Lee DH, Lee MJ, Park BH, et al. Friction Anisotropy-Driven Domain Imaging on Exfoliated Monolayer Graphene. *Science*. 2011;333:607-10.
15. Klemenz A, Pastewka L, Balakrishna SG, Caron A, Bennewitz R, Moseler M. Atomic Scale Mechanisms of Friction Reduction and Wear Protection by Graphene. *Nano Lett*. 2014;14:7145-52.
16. Filleter T, McChesney JL, Bostwick A, Rotenberg E, Emtsev KV, Seyller T, et al. Friction and Dissipation in Epitaxial Graphene Films. *Phys Rev Lett*. 2009;102:086102.
17. Sheehan PE, Lieber CM. Friction between van der Waals Solids during Lattice Directed Sliding. *Nano Lett*. 2017;17:4116-21.
18. Lucas M, Zhang X, Palaci I, Klinke C, Tosatti E, Riedo E. Hindered Rolling and Friction Anisotropy in Supported Carbon Nanotubes. *Nat Mater*. 2009;8:876-81.
19. Cumings J, Zettl A. Low-Friction Nanoscale Linear Bearing Realized from Multiwall Carbon Nanotubes. *Science*. 2000;289(5479):602-4.

20. Chhowalla M, Amaratunga GAJ. Thin Films of Fullerene-like MoS₂ Nanoparticles with ultra-low Friction and Wear. *Nature*. 2000;407:164-7.
21. Zhu H, Wang Y, Xiao J, Liu M, Xiong S, Wong ZJ, et al. Observation of Piezoelectricity in Free-standing Monolayer MoS₂. *Nat Nanotechnol*. 2015;10:151-5.
22. Wu W, Wang L, Li Y, Zhang F, Lin L, Niu S, et al. Piezoelectricity of single-atomic-layer MoS₂ for energy conversion and piezotronics. *Nature*. 2014;514(7523):470-4.
23. Wachter S, Polyushkin DK, Bethge O, Mueller T. A Microprocessor Based on a Two-Dimensional Semiconductor. *Nat Commun*. 2017;8:14948.
24. Leven I, Krepel D, Shemesh O, Hod O. Robust Superlubricity in Graphene/h-BN Heterojunctions. *J Phys Chem Lett*. 2013;4:115-20.
25. Blumberg A, Keshet U, Zaltsman I, Hod O. Interlayer Registry to Determine the Sliding Potential of Layered Metal Dichalcogenides: The Case of 2H-MoS₂. *J Phys Chem Lett*. 2012;3:1936-40.
26. Park JY, Ogletree DF, Thiel PA, Salmeron M. Electronic Control of Friction in Silicon pn Junctions. *Science*. 2006;313:186.
27. Burgo TAL, Silva CA, Balestrin LBS, Galembeck F. Friction Coefficient Dependence on Electrostatic Tribocharging. *Sci Rep*. 2013;3:2384.
28. Li M-Y, Shi Y, Cheng C-C, Lu L-S, Lin Y-C, Tang H-L, et al. Epitaxial Growth of a Monolayer WSe₂-MoS₂ lateral p-n junction with an Atomically Sharp Interface. *Science*. 2015;349:524-8.
29. Perea-López N, Lin Z, Pradhan NR, Iñiguez-Rábago A, Elías AL, McCreary A, et al. CVD-Grown Monolayered MoS₂ as an Effective Photosensor Operating at Low-Voltage. *2D Mater*. 2014;1:011004.
30. van der Zande AM, Huang PY, Chenet DA, Berkelbach TC, You YM, Lee GH, et al. Grains and Grain Boundaries in Highly Crystalline Monolayer Molybdenum Disulphide. *Nat Mater*. 2013;12:554-61.
31. Butt H-J, Jaschke M. Calculation of Thermal Noise in Atomic Force Microscopy. *Nanotechnology*. 1995;6:1-7.
32. Liu W, Bonin K, Guthold M. Easy and Direct Method for Calibrating Atomic Force Microscopy Lateral Force Measurements. *Rev Sci Instrum*. 2007;78:063707.
33. Kim JH, Lee J, Kim JH, Hwang C, Lee C, Park JY. Work Function Variation of MoS₂ Atomic Layers Grown with Chemical Vapor Deposition: The Effects of Thickness and the Adsorption of Water/Oxygen Molecules. *Appl Phys Lett*. 2015;106:251606.
34. Kahn A. Fermi level, work function and vacuum level. *Mater Horiz*. 2016;3:7-10.
35. Riedo E, Lévy F, Brune H. Kinetics of Capillary Condensation in Nanoscopic Sliding Friction. *Phys Rev Lett*. 2002;88:185505.
36. Gavaille J, Takadoum J. Surface Charges and Adhesion Measured by Atomic Force Microscope Influence on Friction Force. *Tribol Int*. 2003;36:865-71.
37. Riedo E, Pallaci I, Boragno C, Brune H. The 2/3 power law dependence of capillary force on normal load in nanoscopic friction. *J Phys Chem B*. 2004;108(17):5324-8.
38. Dai Q, Hu J, Salmeron M. Adsorption of Water on NaCl (100) Surfaces: Role of Atomic Steps. *J Phys Chem B*. 1997;101:1994-8.
39. Ye Z, Balkanci A, Martini A, Baykara MZ. Effect of Roughness on the Layer-Dependent Friction of Few-Layer Graphene. *Phys Rev B*. 2017;96:115401.

40. Jin W, Yeh P-C, Zaki N, Zhang D, Sadowski JT, Al-Mahboob A, et al. Direct Measurement of the Thickness-Dependent Electronic Band Structure of MoS₂ Using Angle-Resolved Photoemission Spectroscopy. *Phys Rev Lett*. 2013;111:106801.
41. Lin Y-K, Chen R-S, Chou T-C, Lee Y-H, Chen Y-F, Chen K-H, et al. Thickness-Dependent Binding Energy Shift in Few-Layer MoS₂ Grown by Chemical Vapor Deposition. *ACS applied materials & interfaces*. 2016;8(34):22637-46.
42. Palermo V, Ridolfi G, Talarico AM, Favaretto L, Barbarella G, Camaioni N, et al. A Kelvin Probe Force Microscopy Study of the Photogeneration of Surface Charges in All - Thiophene Photovoltaic Blends. *Adv Funct Mater*. 2007;17:472-8.
43. Ochedowski O, Bussmann BK, Schleberger M. Graphene on Mica - Intercalated Water Trapped for Life. *Sci Rep*. 2014;4:6003.
44. Lee SY, Kim UJ, Chung J, Nam H, Jeong HY, Han GH, et al. Large Work Function Modulation of Monolayer MoS₂ by Ambient Gases. *ACS nano*. 2016;10:6100-7.
45. Ochedowski O, Marinov K, Scheuschner N, Poloczek A, Bussmann BK, Maultzsch J, et al. Effect of Contaminations and Surface Preparation on the Work Function of Single Layer MoS₂. *Beilstein J Nanotechnol*. 2014;5:291-7.
46. Kraut E, Grant R, Waldrop J, Kowalczyk S. Precise Determination of the Valence-Band Edge in X-Ray Photoemission Spectra: Application to Measurement of Semiconductor Interface Potentials. *Phys Rev Lett*. 1980;44:1620.
47. Choi S, Shaolin Z, Yang W. Layer-Number-Dependent Work Function of MoS₂ Nanoflakes. *J Korean Phys Soc*. 2014;64:1550-5.
48. Kaushik V, Varandani D, Metha BR. Nanoscale Mapping of Layer-Dependent Surface Potential and Junction Properties of CVD-Grown MoS₂ Domains. *J Phys Chem C*. 2015;119:20136-42.
49. Qiu H, Xu T, Wang Z, Ren W, Nan H, Ni Z, et al. Hopping Transport through Defect-induced Localized States in Molybdenum Disulphide. *Nat Commun*. 2013;4:2642.
50. de la Rosa CJL, Nourbakhsh A, Heyne M, Asselberghs I, Huyghebaert C, Radu I, et al. Highly Efficient and Stable MoS₂ FETs with Reversible n-Doping Using a Dehydrated Poly (vinyl-alcohol) Coating. *Nanoscale*. 2017;9:258-65.
51. Park H-Y, Lim M-H, Jeon J, Yoo G, Kang D-H, Jang SK, et al. Wide-range controllable n-doping of molybdenum disulfide (MoS₂) through thermal and optical activation. *ACS nano*. 2015;9(3):2368-76.
52. Lu C-PL, Li G, Mao J, Wang L-M, Andrei EY. Bandgap, Mid-Gap States, and Gating Effects in MoS₂. *Nano Lett*. 2014;14:4628-33.
53. McDonnell S, Addou R, Buie C, Wallace RM, Hinkle CL. Defect-Dominated Doping and Contact Resistance in MoS₂. *ACS nano*. 2014;8:2880-8.
54. Kim J, Byun S, Smith AJ, Yu J, Huang J. Enhanced Electrocatalytic Properties of Transition-Metal Dichalcogenides Sheets by Spontaneous Gold Nanoparticle Decoration. *J Phys Chem Lett*. 2013;4:1227-32.
55. Sadewasser S, Glatzel T, Rusu M, Jäger-Waldau A, Lux-Steiner MC. High-Resolution Work Function Imaging of Single Grains of Semiconductor Surfaces. *Appl Phys Lett*. 2002;80:2979-81.